Published in final edited form as:
Physiol Behav. 2007 November 23; 92(4): 691–701.

LENTIVIRUS-MEDIATED DOWNREGULATION OF HYPOTHALAMIC INSULIN RECEPTOR EXPRESSION

C.A. Grillo[1], **K.L. Tamashiro**[2], **G.G. Piroli**[1], **S. Melhorn**[2], **J.T. Gass**[1], **R.J. Newsom**[1], **L. R. Reznikov**[1], **A. Smith**[1], **S.P. Wilson**[1], **R.R. Sakai**[2], and **L.P. Reagan**[1]

1 *Department of Pharmacology, Physiology & Neuroscience, University of South Carolina, Columbia, SC*

2 *Department of Psychiatry, University of Cincinnati Medical Center, Cincinnati, OH.*

Abstract

Regulation of feeding behavior and energy balance are among the central effects of insulin. For example, intracerebroventricular administration of insulin decreases food intake and body weight, whereas antisense oligodeoxynucleotide downregulation of insulin receptors (IRs) produces hyperphagia. To further examine the role of IRs in the central actions of insulin, we designed an IR antisense lentiviral vector (LV-IRAS) and injected this vector into the third ventricle to selectively decrease IR expression in the rat hypothalamus. Three weeks after LV-IRAS administration, the expression of IRs in the hypothalamus was significantly decreased, whereas no changes were observed in hippocampal IR levels. LV-IRAS administration decreased insulin-stimulated phosphorylation of hypothalamic IRs and translocation of the insulin-sensitive glucose transporter GLUT4 in the hypothalamus; no changes in IR signaling were observed in the hippocampus of LV-IRAS-treated rats. Lentivirus-mediated downregulation of IR expression and signaling produced significant increases in body weight, as well as increases in fat mass that were selective for the subcutaneous compartment. Conversely, lean muscle mass and water mass were not affected in LV-IRAS-treated rats compared to rats treated with control virus. Changes in peripheral adiposity were associated with increases in basal hypothalamic leptin signaling in the absence of changes in leptin receptor expression in LV-IRAS rats. Collectively, these data illustrate the important functional relationships between hypothalamic insulin and leptin signaling in the regulation of body composition and provide insight into the mechanisms through which decreases in IR expression and signaling dysregulates leptin activity, thereby promoting increases in peripheral adiposity.

1. Introduction

The insulin receptor (IR) is a heterotetrameric protein consisting of two extracellular α subunits that provide the insulin-binding domain and two transmembrane-spanning β subunits [1]. Insulin binding stimulates the tyrosine kinase activity of the β subunit, leading to the activation of intracellular signaling events. In peripheral tissues, IR activation stimulates increases in glucose uptake [2]. Cloning and characterization of an insulin-sensitive glucose transporter, GLUT4, helped to elucidate the mechanisms through which IR activation and signaling elicited increases in glucose uptake [3,4]. In particular, IR activation initiates a cascade of events that stimulate the translocation of GLUT4 from an intracellular pool to the plasma membrane,

Correspondence and reprint requests to: Lawrence P. Reagan, Ph.D., Department of Pharmacology, Physiology and Neuroscience, University of South Carolina School of Medicine, 6439 Garner's Ferry Road, D40, Columbia, SC 29208, E-mail: lpreagan@gw.med.sc.edu.

significantly enhancing the ability of peripheral tissues to increase glucose uptake [5]. The IR is also expressed in discrete neuronal populations in the CNS, including the hypothalamus [6,7], where it is proposed to regulate feeding behavior and energy metabolism [8]. For example, intracerebroventricular administration of insulin [9] or insulin mimetics [10] decrease food intake, body weight and peripheral adiposity. Conversely, these measures are increased in IR knockout mice [11] and following downregulation of hypothalamic IRs using antisense oligonucleotide approaches [12]. Collectively, these studies suggest that hypothalamic IRs play an important role in normal physiological processes, as well as in pathological settings such as insulin resistant states and type 2 diabetes.

There are several caveats and limitations associated with these molecular approaches that have examined IR function in the CNS. For example, one potential complication associated with the use of knock-out mice is that compensatory changes may occur during development due to elimination of the gene of interest. This may be particularly relevant to IR expression in the CNS since insulin also exhibits affinity for insulin-like growth factor I (IGF-I) receptor and IGF-I receptors are expressed in the hypothalamus [6]. Administration of antisense oligonucleotides avoids this potential limitation associated with knock-out mice, but requires constant infusion of antisense sequences that may produce short-lived effects. An emerging technology that provides an alternative to these approaches is virus-mediated gene transfer [13]. Virus-mediated gene transfer induces long lasting changes in gene expression in targeted brain regions in adult animals, thereby allowing for examination of the role of a particular gene in neuronal function from the cellular to the behavioral levels. In view of the advantages of this approach, the aim of the current study was to determine the efficacy of virus-mediated gene transfer to examine the functional activities of the IR in the hypothalamus, including examination of the role of central IRs in peripheral body composition and in the translocation of the insulin-sensitive glucose transporter GLUT4. Because of the important relationship between insulin and leptin in modulation of metabolism and body composition [14], we additionally examined the effect of decreasing hypothalamic IRs upon leptin signaling.

2. Materials and methods

2.1. Lentivirus construction

A plasmid containing a 747-bp fragment of the insulin receptor gene, containing 335 bp of the rat insulin receptor coding region plus 124 bp of the adjacent 3′-UTR was generously provided by Dr D. LeRoith (NIH). This DNA fragment was cloned into a lentivirus transfer vector, inserted in antisense orientation relative to the human phosphoglycerate kinase-1 (PGK) promoter. This transfer vector also contained an encephalomyocarditis virus internal ribosome entry site (IRES) and enhanced green fluorescent protein (EGFP). Virus was produced by transfection of human embryonic kidney 293T cells with the transfer vector, a packaging plasmid (pCMV R8.92), a plasmid encoding the rev gene and a plasmid encoding vesicular stomatitis virus G glycoprotein gene. A control virus, LV-Con, was constructed similarly, using a transfer vector with the PGK promoter driving expression of EGFP alone (no IRES).

2.2. Animal Protocols

Adult male Sprague Dawley rats (CD strain, Charles River) weighing 200–250 g were housed in groups of three with *ad libitum* access to food and water, in accordance with all guidelines and regulations of The University of South Carolina Animal Care and Use Committee. Animals were maintained in a temperature-controlled room, with a light/dark cycle of 12/12 h (lights on at 0700h). Rats were handled daily for 5 days and then underwent stereotaxic surgery. Rats were anesthetized, placed in the stereotaxic apparatus and lentivirus was injected into the third ventricle using the following coordinates: AP: −2.6 mm; L: 0.0 mm; DV: −10.0 mm. Rats were injected with lentivirus containing an antisense sequence selective for the IR (LV-IRAS) or

control virus (LV-Con). The viral stock (20,000 tu/ul) was injected at a speed of 1 ul/min with a 10 ul Hamilton syringe driven by a motorized stereotaxic injector (Stoelting 53310); the needle was left in place for additional 10 min. Total volume injected was 4 ul. Rats were returned to the housing colony and sacrificed 21 days after LV administration. Carcasses were sealed in individual plastic bags and frozen at −80° C for later body composition analysis. Oral glucose tolerance test: rats were subjected to an overnight fast; the following morning glucose (2 g/kg) was administered by gastric intubation. Blood samples were collected from the tip of the tail in heparinized tubes at the following time points following intubation: 0 (baseline), 30, 60, 90 and 120 mins. Blood glucose levels were measured by glucose oxidase method (Pointe Scientific, Inc., Canton, MI); plasma insulin levels were measured by ELISA (Linco Research, Inc. St Charles, Missouri). For GLUT4 translocation assays, rats were subjected to an overnight fast; the following morning glucose (2 g/kg) was administered by gastric intubation. Following glucose administration, animals were returned to their home cage. Blood samples were collected from the tip of the tail in heparinized tubes 30, 60 and 90 minutes post-injection for plasma glucose analysis. The brains were quickly removed two hours after glucose administration, the hypothalamus and hippocampus were isolated and stored at −70°C until use.

2.3. Body composition analysis

Body composition of animals was determined by nuclear magnetic resonance (NMR) method (EchoMRI Whole Body Composition Analyzer, Echo Medical Systems, Houston, TX). This method provides estimates of total lean tissue, fat tissue, and water content. Animals (LV-IRAS =14; LV-Con = 13) were additionally processed for determination of fat distribution. In this procedure, all of the skin was gently removed from the carcass, including the fat attached to the skin (including the dorsal subcutaneous and inguinal fat pads), to separate subcutaneous from visceral fat. The skin and attached subcutaneous fat (“subcutaneous depot”) was then analyzed separately from the rest of the body, which contained the organs and visceral fat (“visceral depot”). The two samples were placed in individual plastic freezer bags and frozen at −80° C until analyzed by NMR.

2.4. Membrane preparation

Isolation of membrane-containing fractions was performed as described previously [15,16]. Briefly, hypothalamic or hippocampal punches were weighed, homogenized in ice-cold homogenization buffer and centrifuged for 10 min at 500g at 4°C. Punches were prepared from individual rats for subsequent analyses and were not pooled. Sample sizes consisted of 13 for the LV-IRAS group and 12 for the LV-Con group. The total membrane fraction (supernatant) was saved; a portion of this fraction was centrifuged at 31,000g for 30 mins at 4°C. The resulting pellet, which contained the plasma membrane fraction, was resuspended in PBS. Protein concentrations of the total membrane fraction and the plasma membrane fraction was determined by the method of Bradford [17] using BSA as a standard.

2.5. In vitro phosphorylation assays

In vitro phosphorylation of the insulin receptor was performed as described by Alkon and co-workers [18,19], with the following modifications. Briefly, 50 μg of hypothalamic or hippocampal total membrane fractions were diluted with reaction buffer (50 mM Tris-HCl, pH 7.4; 1 mM $MgCl_2$; 2 mM EGTA; 1x protease inhibitor cocktail [Sigma Chemical Company]; 1x phosphatase inhibitor cocktail [Sigma Chemical Company]). In vitro phosphorylation was stimulated by addition of 1 μM insulin and 5 mM ATP (+ lanes); basal levels of phosphorylation were measured in samples treated with buffer (− lanes). Following addition of insulin/ATP or buffer, samples were incubated for 3 minutes at 37°C. SDS/PAGE sample buffer was quickly

added, the samples were boiled for 10 minutes and added to a precast 4–20% SDS/PAGE gel (Bio-Rad Laboratories).

2.6. Immunoblot analysis

Immunoblot analysis was performed as described in our previous studies [20,21] and was performed upon at least eight individual punches isolated from the hippocampus or hypothalamus of LV-Con or LV-IRAS rats. Briefly, proteins were separated by SDS/PAGE (10%), transferred to nitrocellulose (NC) membranes and blocked in TBS plus 10% non fat dry milk for 60 min. For GLUT4 translocation assays, 40 μg of plasma membrane fractions or 40 μg of whole membrane fractions were added to the SDS/PAGE. For all other proteins, 20 μg of total membrane fractions were added to the SDS/PAGE. NC membranes were incubated with primary antisera (in TBS/5% non fat dry milk), then washed with TBS plus 0.05% Tween 20 (TBST) and incubated with peroxidase-labeled species-specific secondary antibodies. NC membranes were then washed with TBST and developed using enhanced chemiluminescence reagents (ECL, Amersham) as described by the manufacturer. Normalization for protein loading was performed using a mouse monoclonal primary antibody selective for actin (Sigma Chemical Company).

2.7. Immunohistochemistry

Rats were anesthetized and perfused through the ascending aorta sequentially with normal saline (0.9%), followed by 4% paraformaldehyde in 0.1 M phosphate buffer. Rat brain sections were cut on a freezing microtome at a thickness of 40 μM, washed with phosphate buffered saline and then incubated with primary antisera selective for green fluorescent protein (GFP; 1:1,000 dilution; Sigma Chemical). Sections were washed and incubated with species specific biotinylated IgGs (Vector Laboratories, Burlingame, CA). Sections were then washed and incubated with horseradish peroxidase streptavidin (Vector Laboratories, Burlingame, CA), tissue sections were washed and developed with the metal enhanced DAB substrate kit (Pierce, Rockford, IL).

2.8. Fluoro-Jade histochemistry

Fluoro-Jade histochemistry was performed as described by Schmued and co-workers [22] with the following modifications. Briefly, coronal brain sections from LV-Con and LV-IRAS rats were cut at a thickness of 40 μm on a cryostat microtome and mounted on gelatin-coated slides. Since adrenalectomy (ADX) produces degeneration of dentate gyrus granule neurons [23], coronal brain sections from ADX rats were used as positive controls for Fluoro-Jade labeling. Sections were briefly dried and then were washed and incubated with 0.05% potassium permanganate for 15 minutes at room temperature (RT). Slides were again washed and incubated with 0.001% Fluoro-Jade B (Histochem International) in double distilled water. Sections were then washed in HPLC-grade water, dried on a slide warmer, dehydrated with xylenes, and cover-slipped with permount.

2.9. Autoradiographic film analysis and statistical analysis

Computer-assisted microdensitometry of autoradiographic images was determined on the MCID image analysis system (Imaging Research, Inc., St. Catherines, Canada). Microscale ^{14}C standards (Amersham) were exposed on Kodak X-OMAT film and digitized. Grey level/optical density calibrations were performed using a calibrated film strip ladder (Imaging Research, Inc, St. Catherines, Canada) for optical density. Optical density was plotted as a function of microscale calibration values. Statistical analysis was performed using an unpaired t-test with $P < 0.05$ as the criterion for statistical significance.

3. Results

3.1. LV-IRAS administration selectively downregulates IR expression in the hypothalamus

Rats were given intracerebroventricular (icv) injections of the IR (LV-IRAS) construct or the LV-Con construct into the third ventricle to target IRs expressed in the arcuate nucleus of the hypothalamus. Three weeks after LV administration, rats were perfused and the brains were prepared for immunohistochemical analysis using primary antisera selective for green fluorescent protein (GFP). As shown in Figure 1C, LV-mediated expression of GFP was limited to the hypothalamus and was not detected in brain regions rostral (Panels A and B) or caudal (Panel D) of the injection site following third ventricular administration of the LV constructs. Fluoro-Jade histochemistry [22] was performed in order to determine if lentivirus administration produced neuronal damage in the hypothalamus. As a positive control, Fluoro-Jade histochemistry detected degenerating granule neurons in the dentate gyrus (DG) of adrenalectomized rats (Figure 2, ADX). Conversely, no Fluoro-Jade-positive neurons were detected in the hypothalamic regions surrounding the injection site in the third ventricle, including the arcuate nucleus and the ventromedial hypothalamic nucleus (Figure 2, LV). In order to determine the efficacy of the LV-IRAS construct, micropunches were isolated from hypothalamus and hippocampus of LV-IRAS and LV-control treated rats and prepared for western blot analysis using antisera selective for IR-β. In the hypothalamus and hippocampus, IR- β was detected as a single band with the apparent molecular weight of approximately 95 kDa in both LV-Con-treated rats and LV-IRAS-treated rats (Figure 3, Panel A and Panel B, respectively). Autoradiographic image analysis of this 95 kDa band revealed that IR-β expression was significantly downregulated in the hypothalamus of LV-IRAS-treated rats when compared to LV-Con-treated rats (Figure 3, Panel C). However, IR- β protein expression was unchanged in the hippocampus of LV-IRAS-treated rats when compared with LV-Con-treated rats.

3.2. LV-IRAS administration selectively downregulates IR signaling in the hypothalamus

In order to determine the effects of the LV-IRAS construct upon IR functional activities in the CNS, insulin-stimulated phosphorylation of the IR and insulin-stimulated trafficking of GLUT4 were analyzed as measures of IR signaling in the hypothalamus and hippocampus. In vitro phosphorylation of total membrane extracts from the hypothalamus and hippocampus was performed and followed by western blot analysis using primary antisera that recognize the phosphorylated form of the IR. Incubation of hypothalamic total membrane fractions with insulin and ATP produced a robust increase in the phosphorylation state of the IR (Figure 4, Panel A). Autoradiographic analysis revealed that in vitro phosphorylation of the IR was significantly reduced in the hypothalamus of LV-IRAS rats compared to LV-Con rats; phospho-IR levels were similar in hippocampal extracts from LV-IRAS and LV-Con rats (Figure 4, Panel B). As another measure of IR signaling, insulin-stimulated translocation of GLUT4 to the plasma membrane was determined 2 hours following oral glucose administration as described in our previous studies [24]. While total GLUT4 levels were similar in the hypothalamus of LV-Con and LV-IRAS-treated rats (Figure 5, Panel C), insulin-stimulated trafficking of GLUT4 to the plasma membrane was significantly reduced in the hypothalamus of LV-IRAS treated rats when compared with LV-Con-treated rats (Figure 5, Panel B). Total GLUT4 levels and insulin-stimulated trafficking of GLUT4 to the plasma membrane were similar in the hippocampus of both groups of rats (Figure 5).

3.3. Hypothalamic LV-IRAS administration modulates body weight, body composition and plasma leptin levels

In order to determine the effect of downregulating IR expression and signaling in the hypothalamus upon peripheral glucose metabolism, LV-Con and LV-IRAS rats were subjected to an oral glucose tolerance test following an overnight fast. Glucose clearance was nearly

identical in LV-Con and LV-IRAS rats in response to the oral glucose tolerance test (Figure 6, Panel A). In addition, glucose-stimulated increases in plasma insulin levels were similar in LV-IRAS rats when compared with LV-Con rats (Figure 6, Panel B). In agreement with previous studies in neuronal insulin receptor knock-out (NIRKO) mice [11], LV-IRAS rats exhibited significant increases in body weight beginning 12 days following LV administration and continuing for up to 22 days post-injection (Figure 7). As an additional measure of peripheral metabolism, body composition analysis was performed in LV-Con and LV-IRAS rats. While lean muscle mass and water content were similar in both groups, LV-IRAS treated rats exhibited a significant increase in fat mass when compared with LV-Con treated rats (Figure 8). More selective analysis of body composition revealed that LV-IRAS treated rats preferentially increased their subcutaneous fat, while visceral fat levels were similar in LV-IRAS and LV-Con rats (Figure 9, Panel B). Lean muscle mass and water mass in the visceral and subcutaneous compartments were similar in LV-IRAS rats and LV-Con rats (Figure 9, Panel A). Increases in subcutaneous fat were accompanied with increases in plasma leptin levels in LV-IRAS rats (Table 1). Other endocrine parameters, including plasma glucocorticoid, plasma estradiol, and plasma testosterone levels were similar in LV-IRAS rats and LV-Con rats.

3.4. Hypothalamic leptin receptor signaling, but not expression, is altered in LV-IRAS rats

In view of the important functional interactions between hypothalamic insulin and leptin signaling in the regulation of body composition [25,26], we examined components of leptin receptor signaling in the hypothalamus of LV-IRAS rats and LV-Con rats. Leptin receptor expression was unchanged in the hypothalamus of LV-IRAS rats compared with LV-Con rats (Figure 10). Similarly, basal phosphorylation of JAK2 (tyr1007/1008) was unchanged in LV-IRAS and LV-Con rats (data not shown). Conversely, basal levels of the phosphorylated form of Stat3 were significantly increased in the hypothalamus of LV-IRAS-treated rats compared LV-Con rats (Figure 11). In addition to elevated levels of phospho-Stat3, LV-IRAS-treated rats also exhibited increases in SOCS3 expression (Figure 12). All of these parameters of leptin receptor expression and signaling were similar in the hippocampus of LV-IRAS rats when compared with LV-Con rats. Such results suggest that dysregulation in hypothalamic leptin signaling downstream of Stat3/SOCS3 may contribute to increases in peripheral adiposity observed in LV-IRAS rats.

4. Discussion

The results of the current study demonstrate that lentivirus packaged with a selective IR antisense sequence downregulates IR expression and signaling in the hypothalamus without affecting IR expression or signaling in the hippocampus. Virus-mediated gene transfer produced rapid and robust changes in peripheral body composition in that downregulation of hypothalamic IRs increased body adiposity, in particular subcutaneous fat mass, while not affecting lean muscle mass or water composition. Downregulation of IR expression and signaling also produced changes in hypothalamic leptin signaling that are proposed to contribute to leptin resistance [27]. Importantly, lentivirus elicits long-lasting changes that are observed for at least three weeks following administration of the LV-IRAS construct, in keeping with previous studies on the duration of lentivirus-mediated gene expression [28]. These data demonstrate that the LV-IRAS represents a novel experimental approach to examine the mechanistic and functional properties of central IRs.

4.1. Virus-mediated gene transfer

Lentivirus vectors are based on the human immunodeficiency virus, but are multiply attenuated, replication-defective and self-inactivating. The major advantage of these vectors is that they can transduce non-dividing cells such as neurons, making them invaluable for

research on the mammalian brain. The prolonged activity of LV is produced by a single injection, thereby eliminating the need for multiple injections or constant infusion of antisense oligonucleotide sequences [12]. For example, while antisense oligonucleotide approaches effectively modulate hypothalamic IR activity [12], oligonucleotides may produce transient effects. Conversely, in our previous studies in the amygdala [29,30] and the current results in the hypothalamus, LV is highly expressed 21 days post injection. Other studies have revealed that gene expression is modulated up to several months following lentivirus administration [31]. These long-lasting effects of lentivirus administration provide adequate time for behavioral assays to be coupled with neurochemical and neuroanatomical analyses. Another advantage of this technique is that LV administration can be used to induce over-expression or knockdown of gene expression in a single region in the adult CNS, thereby eliminating any potential compensatory changes in gene expression during development that may occur in transgenic or knockout mice. Virus-mediated gene transfer may be applied to a variety of species, including primates [32] and eliminates the potential complication of species-specific responses. In the case of the current study, use of LV-approaches in rats provides for direct comparisons to our previous studies that have examined IR signaling in the rat CNS [16,24, 33,34].

4.2. Identification of neuronal insulin receptor signaling cascades

One area of research that the LV-IRAS approach may be most beneficial is in gaining greater insight into signal transduction cascades activated by insulin in the CNS and how these signaling cascades may contribute to or participate in the central actions of insulin. For example, autophosphorylation of the IR has been identified as the initiation point for IR signaling in peripheral tissues [2] and the current studies demonstrate that LV-IRAS administration downregulates insulin-stimulated phosphorylation of hypothalamic IRs. A more distal endpoint for IR signaling in peripheral tissues is the translocation of GLUT4 from the cytosolic compartment to the plasma membrane. In the CNS, previous studies have demonstrated that plasma membrane association of GLUT4 is reduced in diabetes phenotypes [20,34,35], while physiologically-relevant increases in plasma insulin levels stimulated by glucose administration increases neuronal GLUT4 trafficking [24]. These results suggest that insulin activation of neuronal IRs may mediate these GLUT4 trafficking events. However, insulin also possess high affinity for the IGF-I receptor [1,36], which is more abundantly expressed in some brain regions when compared with the IR [6,37]. Therefore, several receptor systems may be activated by insulin thereby leading to activation of distinct signal transduction cascades in the CNS. The current results demonstrate that downregulation of hypothalamic IRs decreases insulin-stimulated trafficking of GLUT4 to a level similar to those observed in insulinopenic conditions of experimental models of type 1 diabetes [34,35]. Such results suggest that insulin-stimulated trafficking of GLUT4 may be predominantly mediated through the IR, although these findings cannot eliminate a potential role for the IGF-I receptor family. Future investigations using the LV-IRAS construct may provide additional insight into the insulin-stimulated transduction events, as well as how these signaling mechanisms contribute to the central actions of insulin.

We did not detect changes in peripheral glucose uptake following an oral glucose load in LV-IRAS rats when compared with LV-Con rats, suggesting that under these experimental conditions peripheral glucose metabolism is unaffected following downregulation of hypothalamic IRs. Similar findings were reported in male NIRKO mice, in that wild-type (WT) mice and NIRKO mice exhibit similar decreases in blood glucose levels following a peripheral insulin challenge [11]. It is interesting to note that female NIRKO mice exhibited impaired responses to insulin administration when compared to WT female mice. Based upon these observations, as well as the gender differences in adipose tissue distribution (see below), it will be interesting to examine glucose clearance and insulin release in response to an oral glucose

tolerance test in female rats treated with the LV-IRAS construct. Since anti-sense oligonucleotide mediated downregulation of hypothalamic IR expression impairs hepatic insulin activity in male rats [12], it would also be interesting to examine tissue-specific insulin responses following hypothalamic LV-IRAS administration.

4.3. Hypothalamic insulin receptors and body adiposity

Energy homeostasis is under the control of an intricate network of neural and hormonal signals [38,39]. Insulin and leptin are secreted in direct proportion to body fat and administration of either elicits a net catabolic response by altering expression of neuropeptides in the arcuate nucleus, such as neuropeptide Y, agouti-related peptide, and proopiomelanocortin, that are involved in the regulation of energy homeostasis, body composition and food intake. Insulin receptors are located in the medial and lateral portions of the arcuate nucleus of the hypothalamus. Studies show decreased fat mass in response to long term ICV insulin treatment and suggests a critical role for insulin in regulation of body composition [9,40]. Disruption of insulin receptor throughout the brain results in increased body adiposity, plasma insulin and leptin levels [11]. More selective knockdown of insulin receptor expression in the hypothalamus using antisense oligodeoxynucleotides leads to greater adiposity specifically in the subcutaneous depot [12]. Our body composition data are consistent with these data and the preferential increase in subcutaneous fat over visceral fat supports insulin's role in regulation of adipose tissue distribution. In addition to increases in peripheral adiposity, LV-IRAS rats exhibited significant increases in body weight gain beginning 12 days after hypothalamic LV administration, increases that are maintained for the remainder of our 22 day paradigm. Interestingly, female NIRKO mice, but not male NIRKO mice also exhibit changes in body weight when compared with their WT littermates [11]. Since the current studies were performed in male rats, it will be interesting to examine gender differences in body weight following LV-IRAS administration (see below). Unlike the changes we observed in body weight and compostion, we did not detect significant changes in total daily food intake in rats treated with the LV-IRAS construct (data not shown). Nonetheless, based upon the changes in body weight and adiposity, it will be important to examine more discrete measures of feeding behavior, such as meal patterns or meal size.

There are gender differences in distribution of adipose tissue such that males have greater visceral fat depots and female have greater subcutaneous depots [41]. Adipose tissue distribution in males correlates with plasma insulin concentration while in females it corresponds better with leptin levels [42,43]. In addition, male rats are more sensitive to the catabolic action of central insulin compared with females [44] and this difference has been attributed to the actions of gonadal hormones [45]. Intact male rats have less subcutaneous fat compared to females and gonadectomy increases the proportion of subcutaneous fat [46]. In addition, administration of estradiol to intact males shifts adipose deposition toward the subcutaneous depot suggesting that the ratio of estrogen:testosterone plays a more important role in determination of fat distribution [47]. However, body composition changed only in the LV-IRAS group in our study despite similar plasma testosterone and estrogen levels between the LV-IRAS and control group (Table 1). Together these data suggest that increased sensitivity of males to the central effects of insulin may be due to differential sensitivity of the insulin receptor or to changes in expression level of the insulin receptor. We did not examine females in this study; however, the LV technology that we have developed would be ideal for further testing of these types of hypotheses.

4.4. Insulin, leptin and peripheral adiposity

In view of the important functional interactions between insulin and leptin in the regulation of peripheral adiposity, our findings that downregulation of hypothalamic IR expression and signaling modulates hypothalamic leptin signaling is intriguing. Increases in plasma leptin

levels in LV-IRAS rats reflect the increases in peripheral fat composition; however, increases in hypothalamic leptin receptor signaling should also initiate a series of intracellular signaling cascades to reduce fat stores [48]. Under normal physiological conditions, increases in phospho-Stat3 will stimulate SOCS3 transcription; SOCS3 will bind to and inhibit leptin signaling. Leptin resistance may involve the dysregulation of these signaling pathways in the hypothalamus [49]. In the current study, increases in SOCS3 expression are observed concurrently with increased phospho-Stat3 levels in the hypothalamus of LV-IRAS rats, suggesting that increases in SOCS3 is not effectively providing feedback inhibition of the leptin receptor. As such, LV-IRAS rats may serve as an invaluable experimental model to examine the signaling mechanisms associated with leptin resistance. A wide spectrum of changes may contribute to leptin resistance, such as alterations in the expression of peptidergic systems that are intimately involved in food intake, homeostasis and body weight regulation. Indeed, leptin activates the anorexigenic melanocortin system in the hypothalamus, while suppressing the activity of the orexigenic peptides neuropeptide Y and agouti-related protein. Examination of the effect of LV-IRAS administration upon the expression of these peptidergic systems may assist in the identification of additional mechanisms that contribute to leptin resistance.

In summary, lentivirus-mediated downregulation of hypothalamic IRs increases peripheral adiposity and produces changes in leptin signaling that may contribute to leptin resistance. While it is clear that multiple peptidergic and hormonal systems are involved in the regulation of body composition [50], insulin and leptin appear to be critical players in these events. This is particularly relevant in determining how IR expression and activity may be impaired in pathophysiological settings such as diabetes. Indeed, it is becoming increasingly apparent that deficits in central IR signaling may also contribute to the peripheral complications of diabetes phenotypes. Since less is known regarding IR signaling in the CNS when compared with the periphery, future investigations using the LV-IRAS construct could begin to address how deficits in central IR signaling contribute to the deleterious consequences of diabetes in the periphery and the CNS.

Acknowledgements

Supported by the Juvenile Diabetes Research Foundation (LPR), and NIH grant numbers DK066596 (RRS) and NS047728 (LPR).

References

1. Jones JI, Clemmons DR. Insulin-like growth factors and their binding proteins: biological actions. Endocr Rev 1995;16:3–34. [PubMed: 7758431]
2. Saltiel AR, Pessin JE. Insulin signaling pathways in time and space. Trends Cell Biol 2002;12:65–71. [PubMed: 11849969]
3. Charron MJ, Brosius FC III, Alper SL, Lodish HF. A glucose transport protein expressed predominately in insulin-responsive tissues. Proc Natl Acad Sci U S A 1989;86:2535–39. [PubMed: 2649883]
4. Birnbaum MJ. Identification of a novel gene encoding an insulin-responsive glucose transporter protein. Cell 1989;57:305–15. [PubMed: 2649253]
5. Shepherd PR, Kahn BB. Glucose transporters and insulin action. Implications for insulin resistance and diabetes mellitus. New Eng J Med 1999;341:248–57. [PubMed: 10413738]
6. Kar S, Chabot J-G, Quirion R. Quantitative autoradiographic localization of [^{125}I]Insulin-like growth factor I, [^{125}I]Insulin-like growth factor II and [^{125}I]Insulin binding sites in developing and adult rat brain. J Comp Neurol 1993;333:375–97. [PubMed: 8349849]
7. Marks JL, Porte D Jr, Stahl WL, Baskin DG. Localization of insulin receptor mRNA in rat brain by in situ hybridization. Endocrinology 1991;127:3234–36. [PubMed: 2249648]
8. Schwartz MW, Figlewicz DP, Baskin DG, Woods SC, Porte D Jr. Insulin in the brain: A hormonal regulator of energy balance. Endocr Rev 1992;13:387–414. [PubMed: 1425482]

9. Woods SC, Lotter EC, McKay LD, Porte D Jr. Chronic intracerebroventricular infusion of insulin reduces food intake and body weight of baboons. Nature 1979;282:503–5. [PubMed: 116135]
10. Air EL, Strowski MZ, Benoit SC, Conarello SL, Salituro GM, Guan XM, Liu K, Woods SC, Zhang BB. Small molecule insulin mimetics reduce food intake and body weight and prevent development of obesity. Nat Med 2002;8:179–83. [PubMed: 11821903]
11. Bruning JC, Gautam D, Burks DJ, Gillette J, Schubert M, Orban PC, Klein R, Krone W, Muller-Wieland D, Kahn CR. Role of brain insulin receptor in control of body weight and reproduction. Science 2000;289:2122–25. [PubMed: 11000114]
12. Obici S, Feng Z, Karkanias G, Baskin DG, Rossetti L. Decreasing hypothalamic insulin receptors causes hyperphagia and insulin resistance in rats. Nat Neurosci 2002;5:566–72. [PubMed: 12021765]
13. Wilson SP, Yeomans DC. Virally mediated delivery of enkephalin and other neuropeptide transgenes in experimental pain models. Ann N Y Acad Sci 2002;971:521.
14. Schwartz MW, Woods SC, Porte D Jr, Seeley RJ, Baskin DG. Central nervous system control of food intake. Nature 2000;404:661–71. [PubMed: 10766253]
15. Reagan LP, Magariños AM, Yee DK, Szweda LI, Van Bueren A, McCall AL, McEwen BS. Oxidative stress and HNE conjugation of GLUT3 are increased in the hippocampus of diabetic rats subjected to stress. Brain Res 2000;862:292–300. [PubMed: 10799703]
16. Piroli GG, Grillo CA, Hoskin EK, Znamensky V, Katz EB, Milner TA, McEwen BS, Charron MJ, Reagan LP. Peripheral glucose administration stimulates the translocation of GLUT8 glucose transporter to the endoplasmic reticulum in the rat hippocampus. J Comp Neurol 2002;452:103–14. [PubMed: 12271485]
17. Bradford MA. A rapid and sensitive method for the quantitation of microgram quantities of protein utilizing the principle of protein-dye binding. Anal Biochem 1976;72:248–54. [PubMed: 942051]
18. Zhao W, Chen H, Moore E, Meiri N, Quon MJ, Alkon DL. Brain insulin receptors and spatial memory. J Biol Chem 1999;274:34893–902. [PubMed: 10574963]
19. Zhao WQ, Alkon DL. Role of insulin and insulin receptor in learning and memory. Mol Cell Endocrinol 2001;177:125–34. [PubMed: 11377828]
20. Winocur G, Greenwood CE, Piroli GG, Grillo CA, Reznikov LR, Reagan LP, McEwen BS. Memory Impairment in Obese Zucker Rats: An Investigation of Cognitive Function in an Animal Model of Insulin Resistance and Obesity. Behav Neurosci 2005;119:1389–95. [PubMed: 16300445]
21. Grillo CA, Piroli GG, Wood GE, Reznikov LR, McEwen BS, Reagan LP. Immunocytochemical analysis of synaptic proteins provides new insights into diabetes-mediated plasticity in the rat hippocampus. Neuroscience. 2005in press
22. Schmued LC, Hopkins KJ. Fluoro-Jade B: a high affinity fluorescent marker for the localization of neuronal degeneration. Brain Res 2000;874:123–30. [PubMed: 10960596]
23. Sloviter RS, Valiquette G, Abrams GM, Ronk EC, Sollas AL, Paul LA, Neubort S. Selective loss of hippocampal granule cells in the mature rat brain after adrenalectomy. Science 1989;243:535–38. [PubMed: 2911756]
24. McEwen BS, Reagan LP. Glucose transporter expression in the central nervous system: relationship to synaptic function. Eur J Pharmacol 2004;490:13–24. [PubMed: 15094070]
25. Schwartz MW, Woods SC, Porte D Jr, Seeley RJ, Baskin DG. Central nervous system control of food intake. Nature 2000;404:661–71. [PubMed: 10766253]
26. Elmquist JK, Coppari R, Balthasar N, Ichinose M, Lowell BB. Identifying hypothalamic pathways controlling food intake, body weight, and glucose homeostasis. J Comp Neurol 2005;493:63–71. [PubMed: 16254991]
27. Munzberg H, Myers MG Jr. Molecular and anatomical determinants of central leptin resistance. Nat Neurosci 2005;8:566–70. [PubMed: 15856064]
28. de Almeida LP, Zala D, Aebischer P, Deglon N. Neuroprotective effect of a CNTF-expressing lentiviral vector in the quinolinic acid rat model of Huntington's disease. Neurobiol Dis 2001;8:433–46. [PubMed: 11442352]
29. Kang W, Wilson SP, Wilson MA. Changes in nociceptive and anxiolytic responses following herpes virus-mediated preproenkephalin overexpression in rat amygdala are naloxone-reversible and transient. Ann N Y Acad Sci 1999;877:751–55. [PubMed: 10415698]

30. Primeaux SD, Wilson SP, Cusick MC, York DA, Wilson MA. Effects of altered amygdalar neuropeptide Y expression on anxiety-related behaviors. Neuropsychopharmacology 2005;30:1589–97. [PubMed: 15770236]

31. de Almeida LP, Zala D, Aebischer P, Deglon N. Neuroprotective effect of a CNTF-expressing lentiviral vector in the quinolinic acid rat model of Huntington's disease. Neurobiol Dis 2001;8:433–46. [PubMed: 11442352]

32. Kordower JH, Bloch J, Ma SY, Chu Y, Palfi S, Roitberg BZ, Emborg M, Hantraye P, Deglon N, Aebischer P. Lentiviral gene transfer to the nonhuman primate brain. Exp Neurol 1999;160:1–16. [PubMed: 10630186]

33. Piroli, GG.; Grillo, CA.; Reznikov, LR.; Reagan, LP. Expression and Functional Activities of Glucose Transporters in the Central Nervous System. In: Lajtha, A., editor. Handbook of Neurochemistry and Molecular Neurobiology. 11. Springer; New York: 2005. in press

34. Reagan LP. Neuronal insulin signal transduction mechanisms in diabetes phenotypes. Neurobiol Aging 2005;26 (Suppl 1):56–59. [PubMed: 16225964]

35. Vannucci SJ, Koehler-Stec EM, Li K, Reynolds TH, Clark R, Simpson IA. GLUT4 glucose transporter expression in rodent brain: effects of diabetes. Brain Res 1998;797:1–11. [PubMed: 9630471]

36. LeRoith D, Adamo M, Werner H, Roberts CT Jr. Insulinlike growth factors and their receptors as growth regulators in normal physiology and pathologic states. Trends Endocrinol Metab 1991;2:134–39.

37. Doré S, Kar S, Rowe W, Quirion R. Distribution and levels of [^{125}I]IGF-I, [^{125}I]IGF-II and [^{125}I] Insulin receptor binding sites in the hippocampus of aged memory-unimpaired and -impaired rats. Neuroscience 1997;80:1033–40. [PubMed: 9284058]

38. Woods SC, Seeley RJ, Porte D Jr, Schwartz MW. Signals that regulate food intake and energy homeostasis. Science 1998;280:1378–83. [PubMed: 9603721]

39. Schwartz MW, Woods SC, Porte D Jr, Seeley RJ, Baskin DG. Central nervous system control of food intake. Nature 2000;404:661–71. [PubMed: 10766253]

40. Sipols AJ, Baskin DG, Schwartz MW. Effect of intracerebroventricular insulin infusion on diabetic hyperphagia and hypothalamic neuropeptide gene expression. Diabetes 1995;44:147–51. [PubMed: 7859932]

41. Wajchenberg BL. Subcutaneous and visceral adipose tissue: their relation to the metabolic syndrome. Endocr Rev 2000;21:697–738. [PubMed: 11133069]

42. Cigolini M, Seidell JC, Targher G, Deslypere JP, Ellsinger BM, Charzewska J, Cruz A, Bjorntorp P. Fasting serum insulin in relation to components of the metabolic syndrome in European healthy men: the European Fat Distribution Study. Metabolism 1995;44:35–40. [PubMed: 7854162]

43. Dua A, Hennes MI, Hoffmann RG, Maas DL, Krakower GR, Sonnenberg GE, Kissebah AH. Leptin: a significant indicator of total body fat but not of visceral fat and insulin insensitivity in African-American women. Diabetes 1996;45:1635–37. [PubMed: 8866572]

44. Clegg DJ, Riedy CA, Smith KA, Benoit SC, Woods SC. Differential sensitivity to central leptin and insulin in male and female rats. Diabetes 2003;52:682–87. [PubMed: 12606509]

45. Clegg DJ, Brown LM, Woods SC, Benoit SC. Gonadal hormones determine sensitivity to central leptin and insulin. Diabetes 2006;55:978–87. [PubMed: 16567519]

46. Clegg DJ, Brown LM, Woods SC, Benoit SC. Gonadal hormones determine sensitivity to central leptin and insulin. Diabetes 2006;55:978–87. [PubMed: 16567519]

47. Clegg DJ, Brown LM, Woods SC, Benoit SC. Gonadal hormones determine sensitivity to central leptin and insulin. Diabetes 2006;55:978–87. [PubMed: 16567519]

48. Schwartz MW, Woods SC, Porte D Jr, Seeley RJ, Baskin DG. Central nervous system control of food intake. Nature 2000;404:661–71. [PubMed: 10766253]

49. Bates SH, Myers MG Jr. The role of leptin receptor signaling in feeding and neuroendocrine function. Trends Endocrinol Metab 2003;14:447–52. [PubMed: 14643059]

50. Berthoud HR. Multiple neural systems controlling food intake and body weight. Neurosci Biobehav Rev 2002;26:393–428. [PubMed: 12204189]

51. Paxinos, G.; Watson, C. The rat brain in sterotaxic coordinates. Academic Press; 1998.

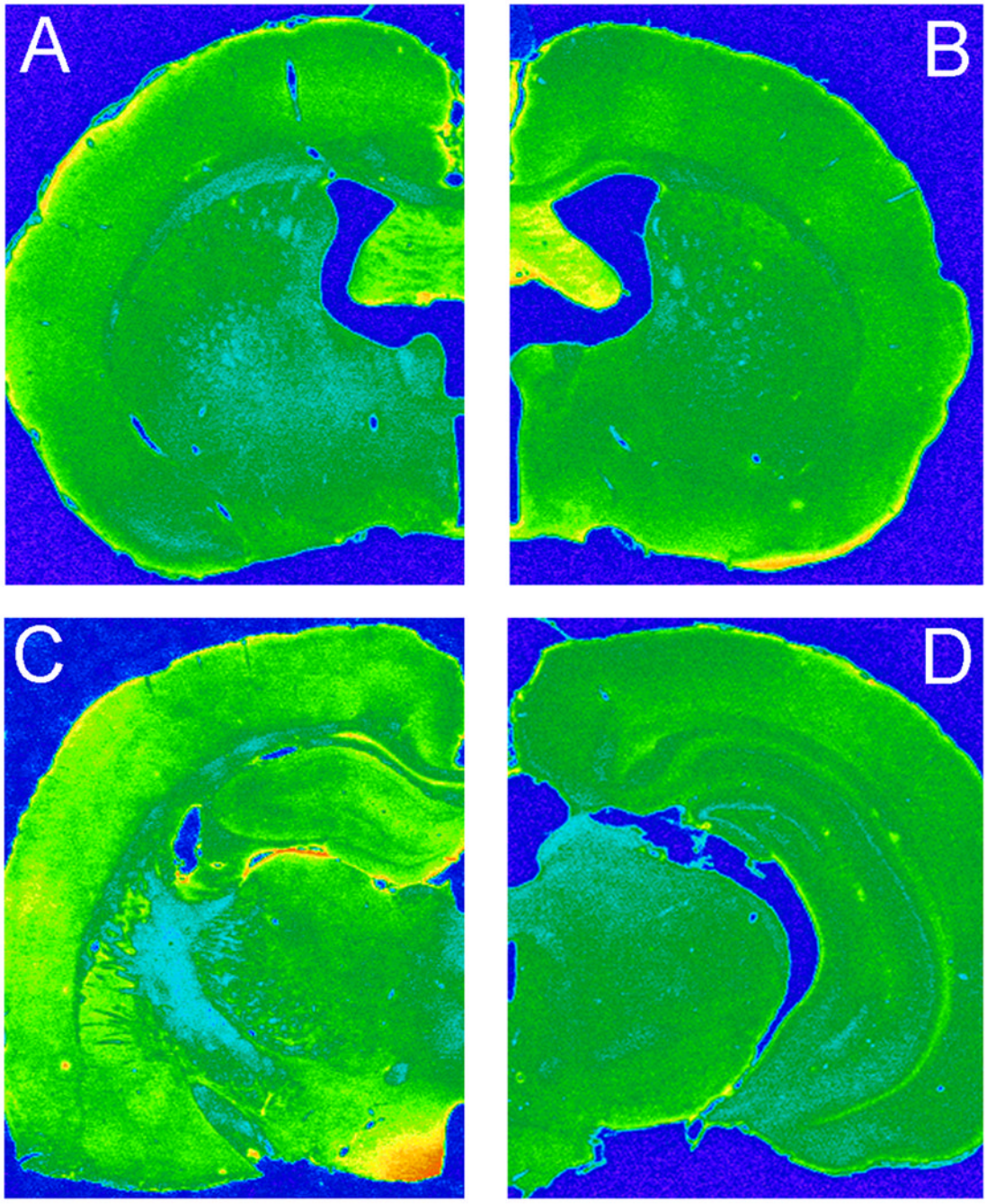

Figure 1.
Representative pseudo-color photomicrograph of GFP immuoreactivity three weeks following third ventricle administration of lentivirus. Lentivirus spread is limited to the hypothalamus and is not detected in other neuronal regions rostral or caudal of the injection site; see Materials and Methods for injection coordinates. [Panel A: Bregma −0.92 mm; Panel B: Bregma −1.30 mm; Panel C: Bregma −2.6; Panel D: Bregma −5.6. All according to atlas of Paxinos and Watson [51]]

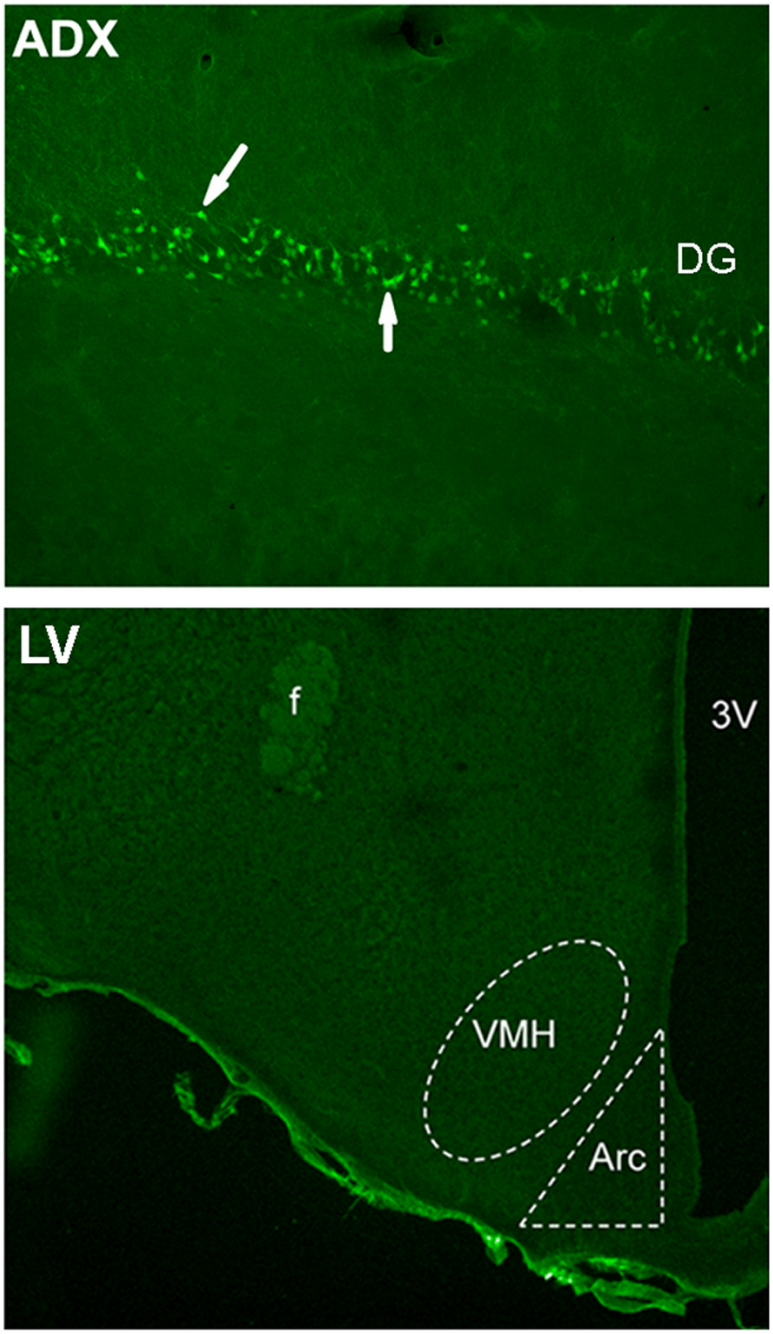

Figure 2.
Fluoro-Jade histochemistry does not detect degenerating neurons in the hypothalamus of LV-treated rats. Fluoro-Jade-positive neurons are detected in the granule cell layer of the dentate gyrus (DG) in adrenalectomized (ADX) rats, as indicated by arrows. Fluoro-Jade labeling is not detected in the arcuate nucleus (Arc) or the ventromedial hypothalamic nucleus (VMH) in rats injected with the lentivirus construct into the third ventricle (LV). [3V: third ventricle; f: fornix]

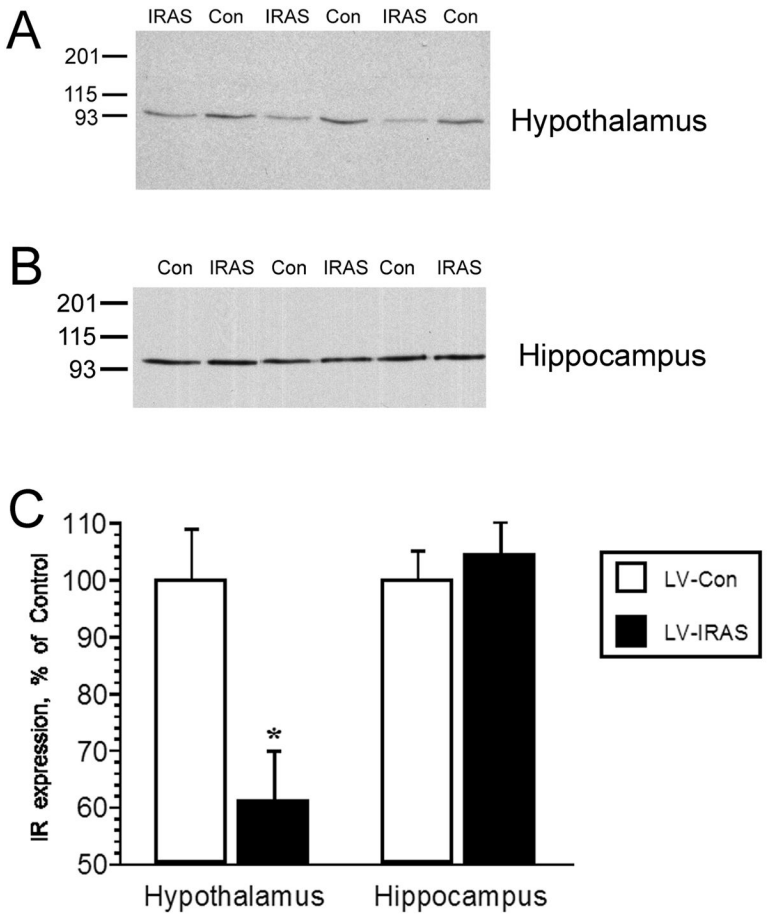

Figure 3.

Selective downregulation of insulin receptor (IR) expression in the hypothalamus three weeks following administration of LV-IRAS construct. Panel A. Representative immunoblot of insulin receptor (IR) expression in the hypothalamus of LV-Con treated and LV-IRAS treated rats. Blot shows hypothalamic IR immunoreactivity from three LV-Con rats and three LV-IRAS rats. Panel B. Representative immunoblot of insulin receptor (IR) expression in the hippocampus of LV-Con treated and LV-IRAS treated rats. Blot shows hippocampal IR immunoreactivity from three LV-Con rats and three LV-IRAS rats. Panel C. Autoradiographic analysis determined that IR expression is significantly decreased in the hypothalamus of LV-IRAS treated rats compared to LV-Con treated rats. Conversely, hippocampal IR expression was unaffected by LV administration. [* = $p \leq 0.001$. Molecular weight standards are shown on left. IR primary antisera from Santa Cruz Biotechnology: #sc-711]

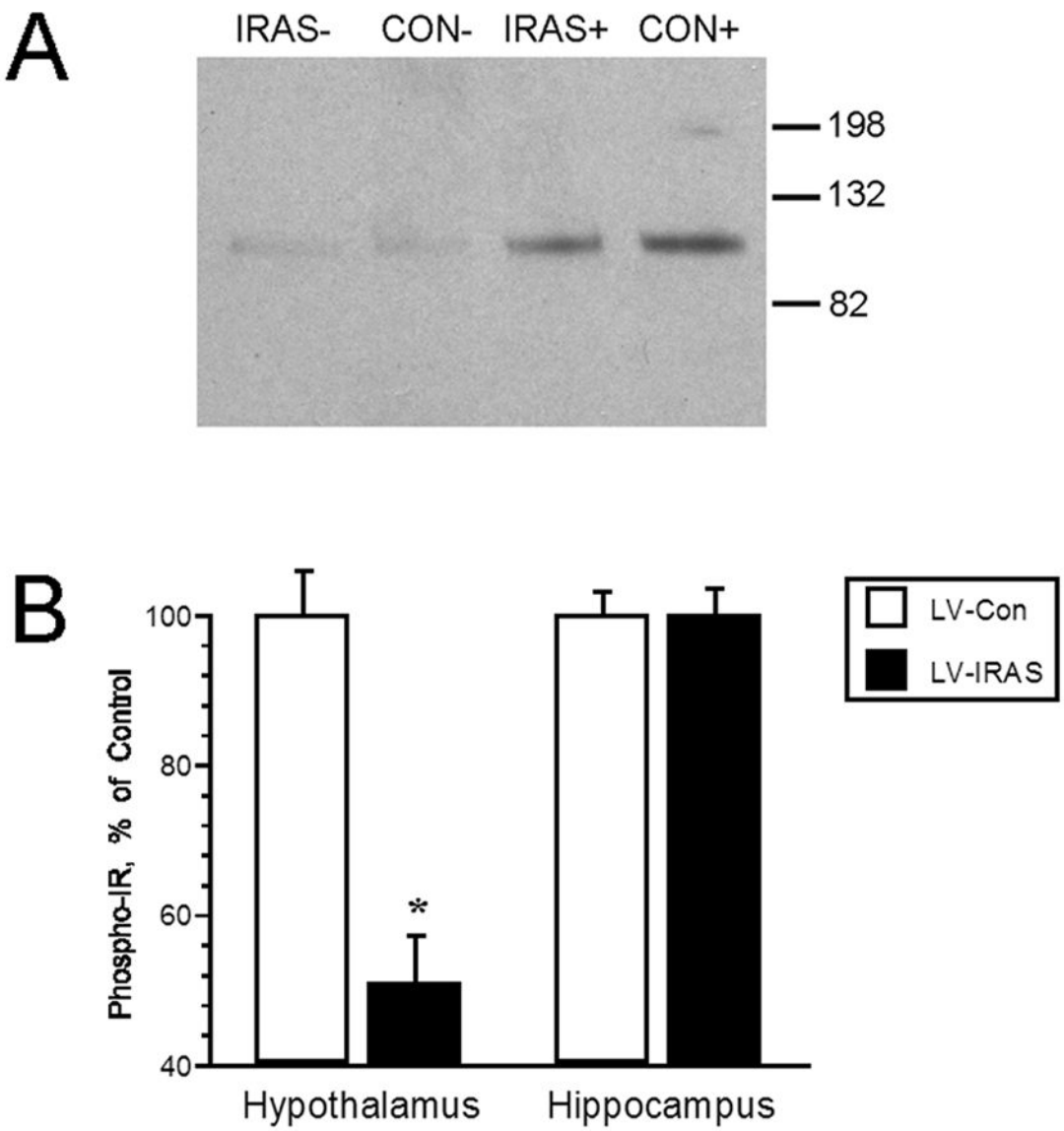

Figure 4.

Insulin-stimulated phosphorylation of the insulin receptor (IR) is decreased in the hypothalamus of LV-IRAS treated rats. Panel A. Representative immunoblot of phospho-IR levels in the hypothalamus of LV-Con and LV-IRAS treated rats. Panel B. Autoradiographic analysis determined that phospho-IR levels are significantly decreased in the hypothalamus of LV-IRAS treated rats compared to LV-Con treated rats. Hippocampal phospho-IR levels are similar in LV-Con and LV-IRAS rats. [* = $p \leq 0.0005$; molecular weight standards are shown on right. + = insulin + ATP treatment; − = buffer treatment. Phospho-IR primary antisera from Cell Signaling Technology: #3021]

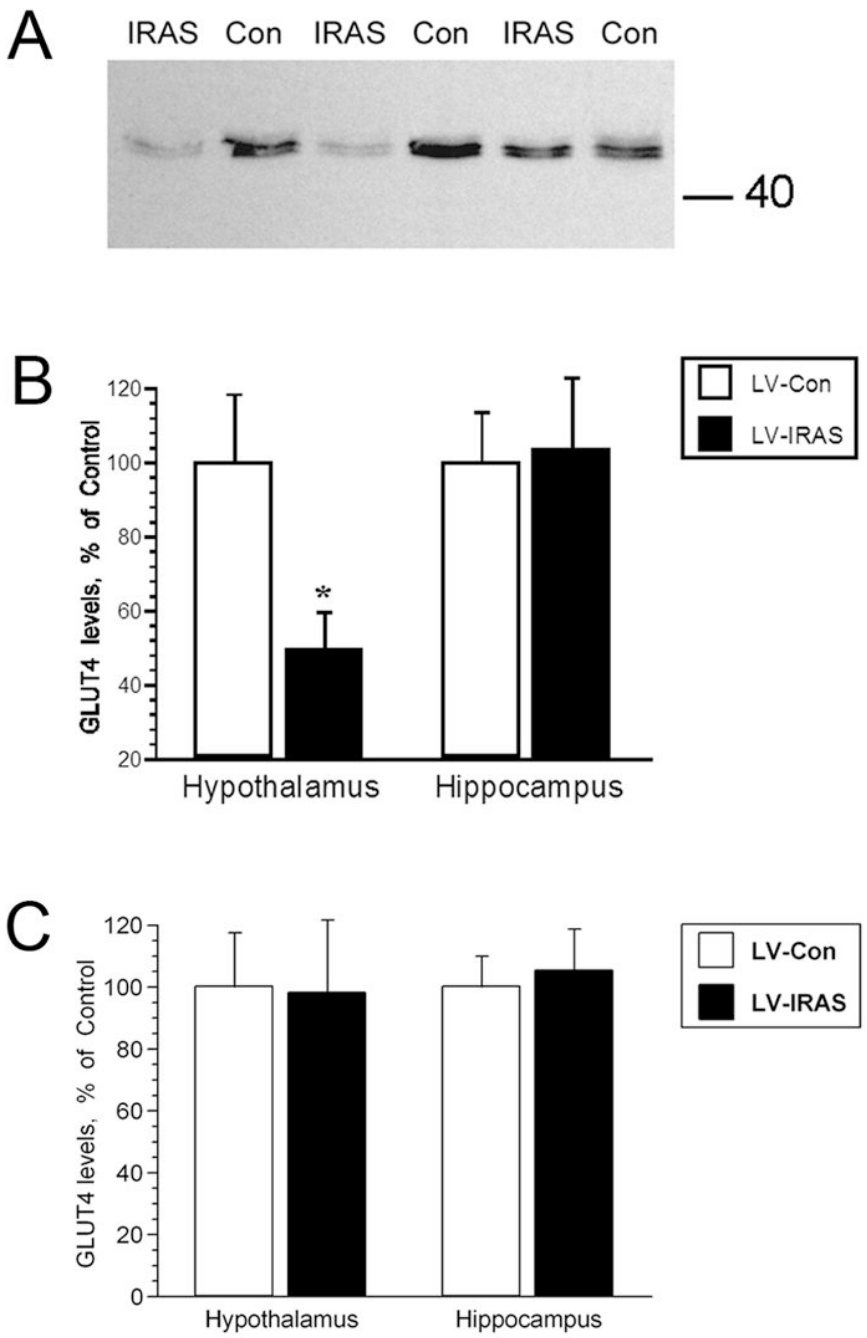

Figure 5.

Insulin-stimulated of GLUT4 translocation to the plasma membrane is decreased in the hypothalamus of LV-IRAS treated rats. Panel A. Representative immunoblot of GLUT4 levels in hypothalamic plasma membrane fractions from LV-IRAS rats and LV-Con rats 2 hours following glucose administration. Blot shows hypothalamic GLUT4 plasma membrane immunoreactivity from three LV-Con and three LV-IRAS rats. Panel B. Autoradiographic analysis determined that plasma membrane association of GLUT4 is significantly decreased in the hypothalamus of LV-IRAS treated rats compared to LV-Con treated rats. GLUT4 levels are similar in plasma membrane fractions isolated from the hippocampus of LV-Con rats and LV-IRAS treated rats. Panel C: Total GLUT4 levels are unchanged in the hypothalamus and

hippocampus of LV-IRAS rats when compared to LV-Con rats. [* = $p \leq 0.05$. Molecular weight standards are shown on right]

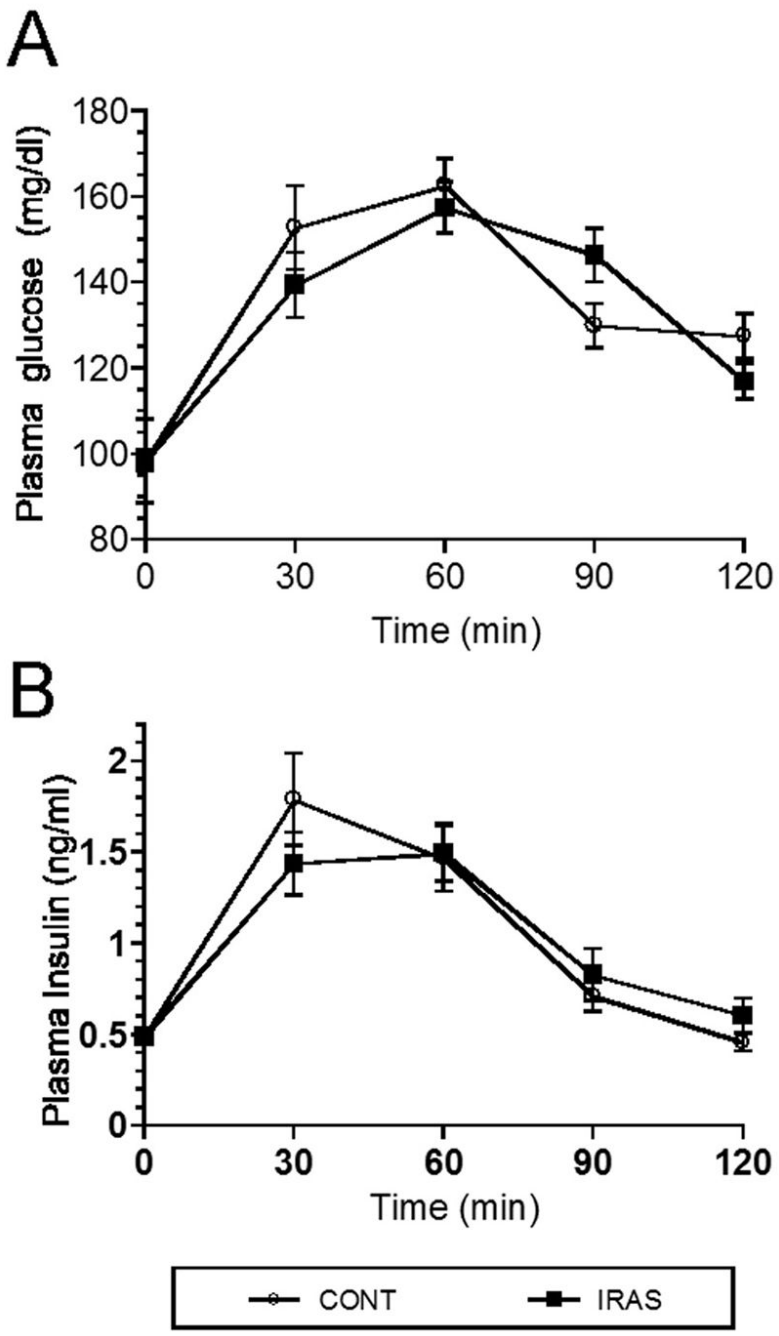

Figure 6.

LV-IRAS administration does not modulate glucose clearance or glucose stimulated insulin release. Panel A. LV-Cont and LV-IRAS rats exhibited similar profiles of glucose clearance in response to oral glucose administration. Panel B. Glucose stimulated increases in plasma insulin levels were similar in LV-IRAS rats when compared with LV-Con rats. Plasma glucose data expressed as mg/dl; plasma insulin levels expressed as ng/ml.

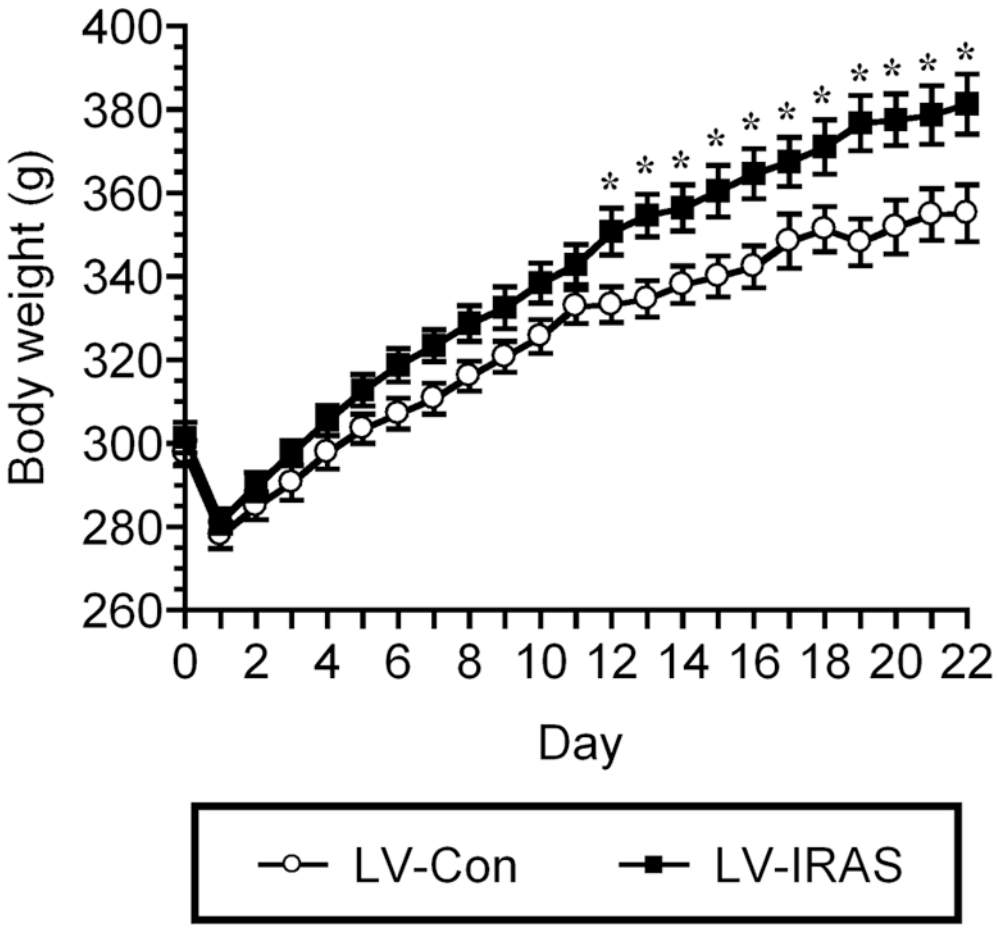

Figure 7.
LV-IRAS-treated rats exhibit significant increases in body weight when compared with LV-Con-treated rats. Both LV-Con and LV-IRAS rats exhibit similar post-operative decreases in body weight. Beginning twelve days following administration, LV-IRAS rats exhibit significant increases in body weight for the remainder of the 22 day paradigm. [* = $p \leq 0.05$]

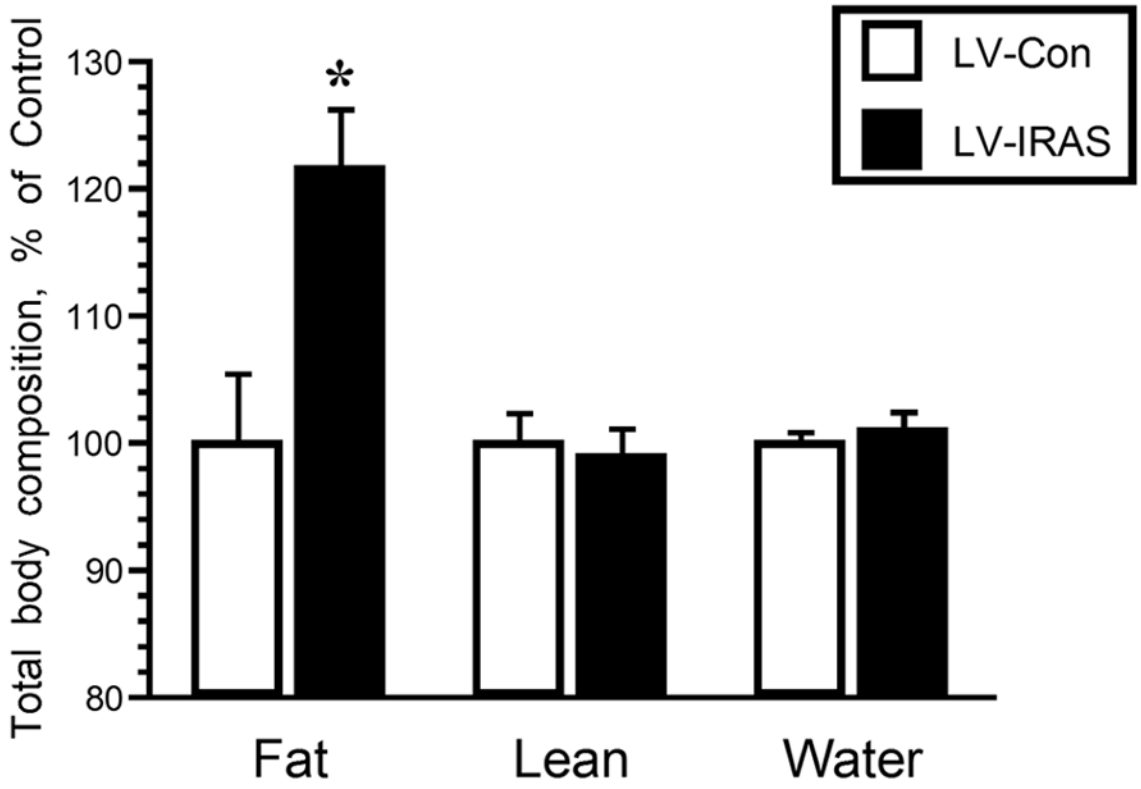

Figure 8.
LV-IRAS administration significantly increases peripheral adiposity. Three weeks after LV administration, total body adiposity is significantly increased in LV-IRAS treated rats compared to LV-Con rats. Total lean muscle mass and water mass were similar in LV-Con and LV-IRAS rats. [* = $p \leq 0.005$]

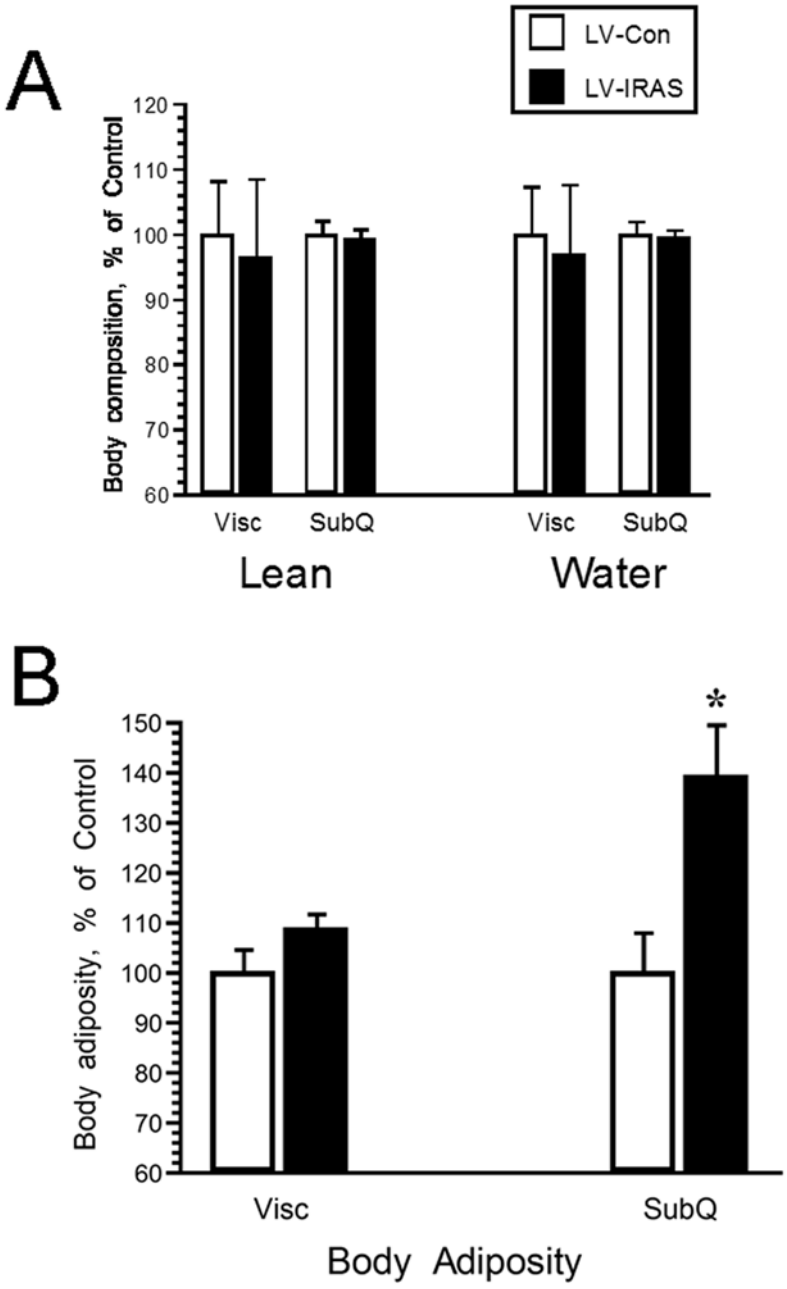

Figure 9.

LV-IRAS administration preferentially increases subcutaneous fat composition. Three weeks after LV administration, subcutaneous fat is significantly increased in LV-IRAS treated rats compared to LV-Con rats. Visceral fat, as well as lean muscle mass and water mass in the visceral and subcutaneous compartments were similar in LV-Con and LV-IRAS rats. [* = $p \leq 0.01$]

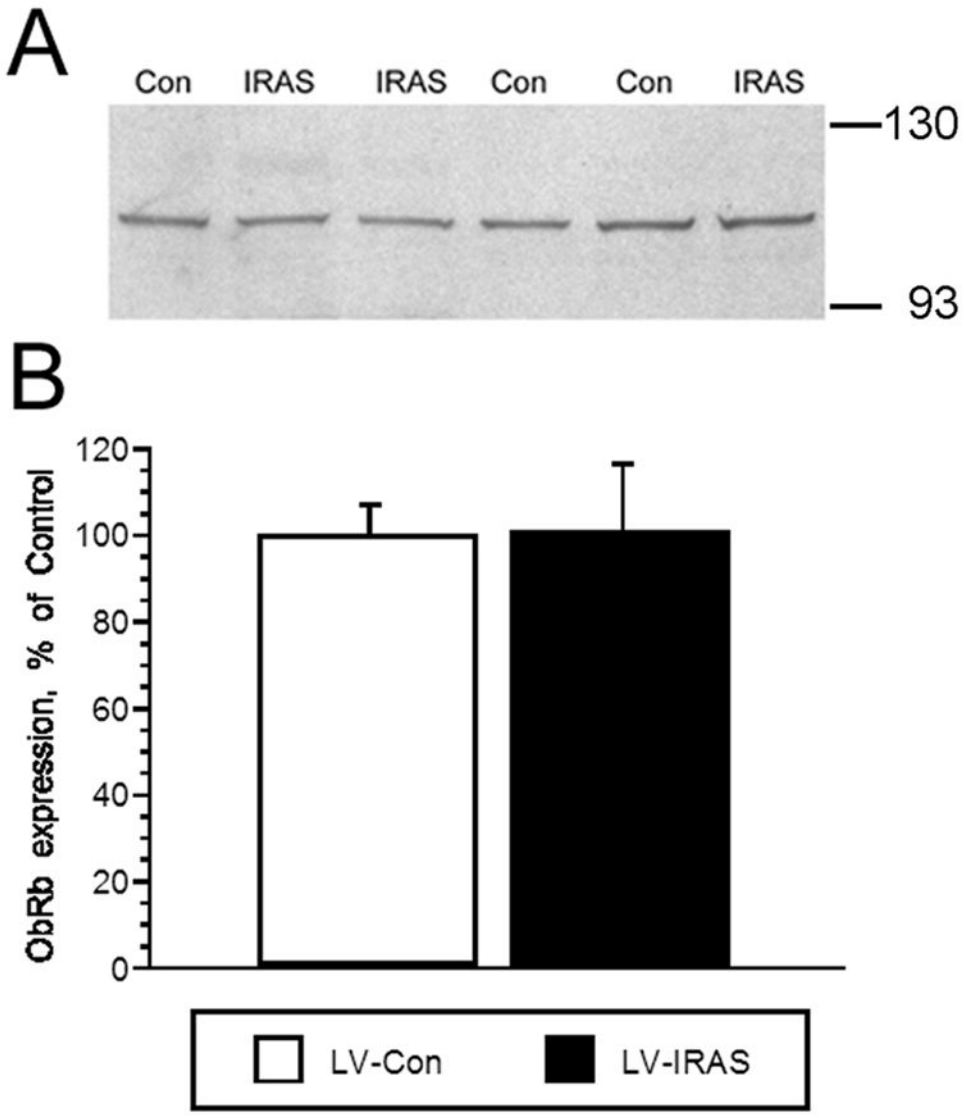

Figure 10.

LV-IRAS administration does not modulate leptin receptor expression in the rat hypothalamus. Panel A. Representative immunoblot of leptin receptor expression in the hypothalamus of LV-IRAS-treated (IRAS) and LV-Con-treated (Con) rats. Panel B. Autoradiographic image analysis revealed that leptin receptor levels are similar in total membrane fractions isolated from the hypothalamus of IRAS and Control rats. [Leptin receptor primary antisera from Santa Cruz Biotechnology: #sc-1834. Molecular weight standards are shown on right]

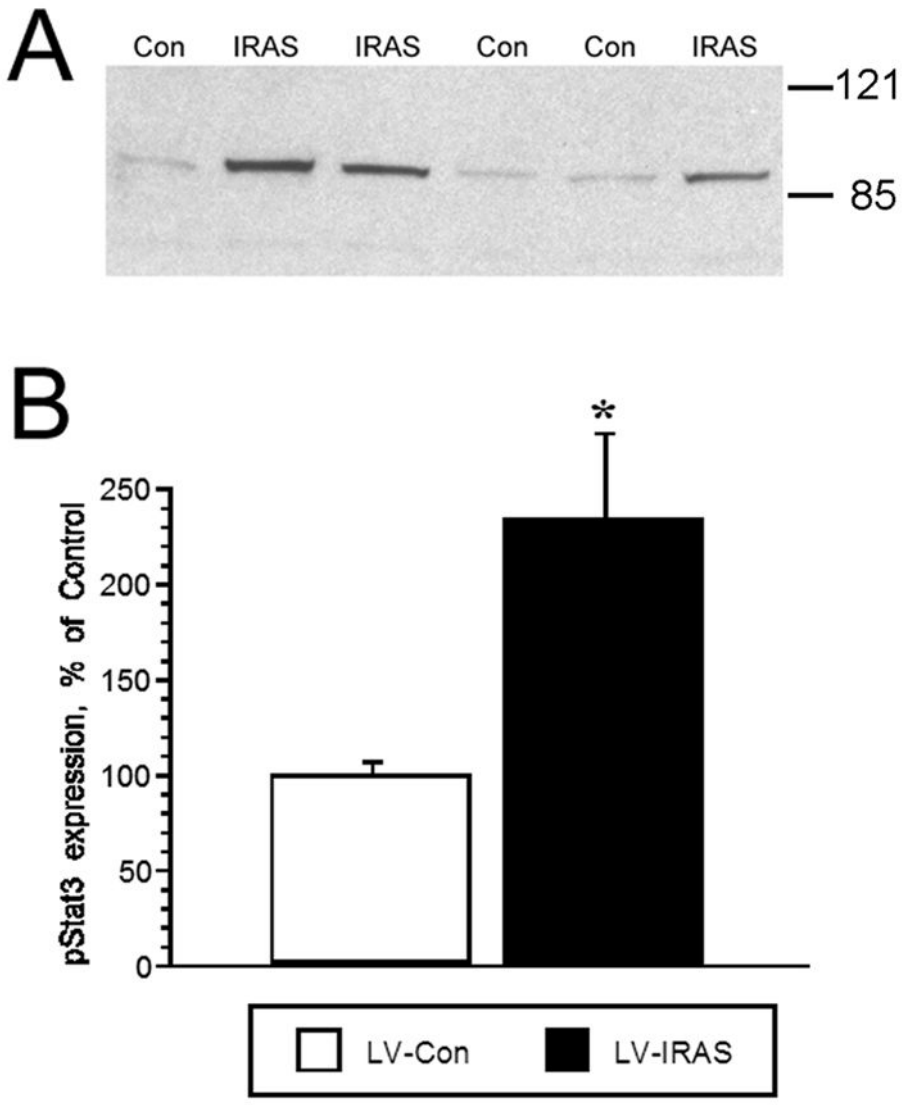

Figure 11.
LV-IRAS administration increases phospho-Stat3 levels in the rat hypothalamus. Panel A: Representative immunoblot of basal phospho-Stat3 levels in total membrane fractions isolated from the hypothalamus of LV-IRAS-treated (IRAS) and LV-Con-treated (Con) rats. Panel B: Autoradiographic image analysis revealed that phospho-Stat3 levels were significantly increased in the hypothalamus of LV-IRAS rats compared with LV-Con rats. [* = $p \leq 0.01$. Phospho-Stat3 primary antisera from Cell Signaling Technology: #9131. Molecular weight standards are shown on right]

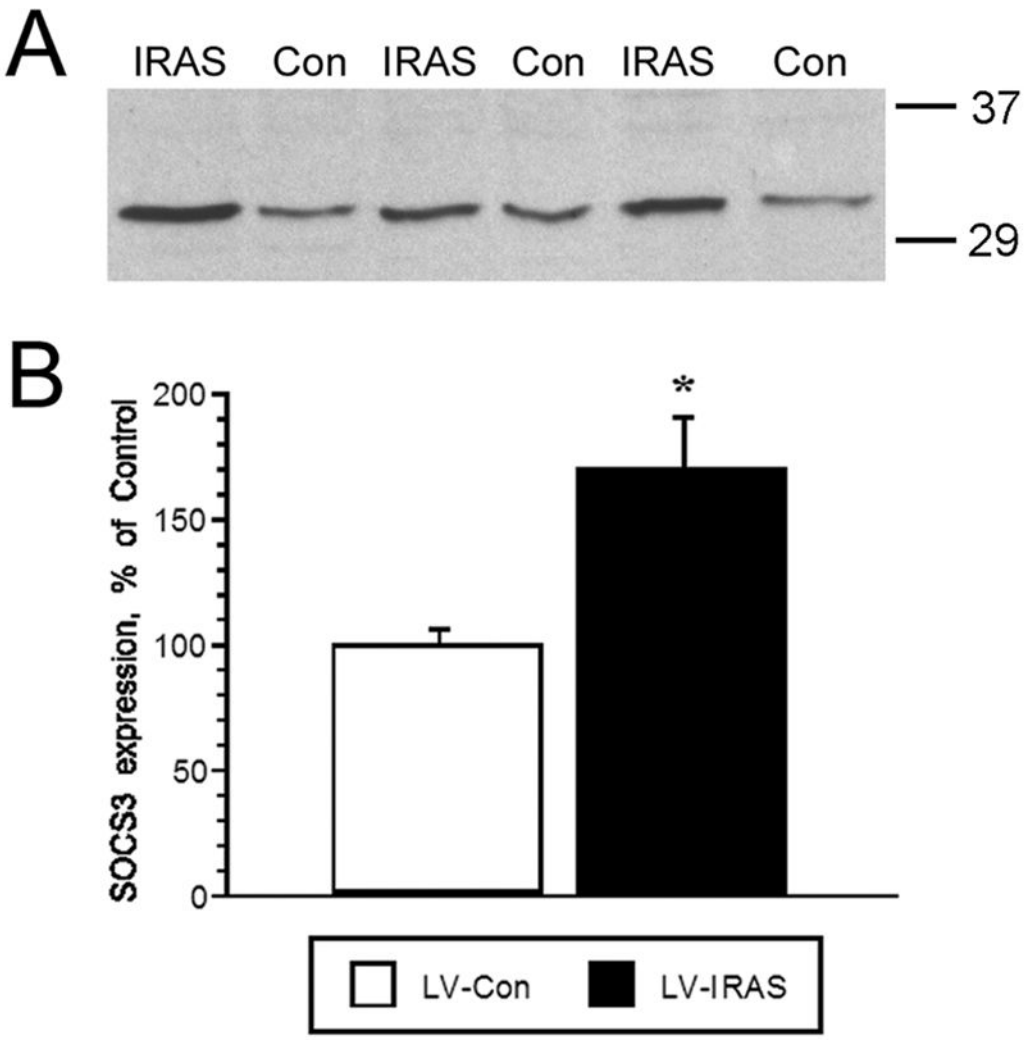

Figure 12.
LV-IRAS administration increases SOCS3 levels in the rat hypothalamus. Panel A: Representative immunoblot of SOCS3 levels in total membrane fractions isolated from the hypothalamus of LV-IRAS-treated (IRAS) and LV-Con-treated (Con) rats. Panel B: Autoradiographic image analysis revealed that SOCS expression is significantly increased in the hypothalamus of LV-IRAS rats compared with LV-Con rats. [* = $p \leq 0.01$; SOCS3 primary antisera from Santa Cruz Biotechnology: #sc-9023. Molecular weight standards are shown on right].

Table 1

Endocrine parameters of LV-Con rats and LV-IRAS rats.

	LV-Con	LV-IRAS	p
Glucose (mg/dl)	98.3 ± 9.8	98.5 ± 2.3	0.986
Insulin (ng/ml)	0.485 ± .0.044	0.489 ± 0.036	0.948
Leptin (ng/ml)	1.03 ± 0.134	1.575 ± 0.199	0.043
Adiponectin (ng/ml)	2.58 ± 0.25	3.89 ± 0.76	0.144
Corticosterone (ng/ml)	35.6 ± 7.2	31.3 ± 8.1	0.701
Estradiol (pg/ml)	20.71 ± 3.42	22.11 ± 4.07	0.799
T-Testosterone (ng/dl)	621.5 ± 145.2	589.8 ± 144.7	0.914
F-Testosterone (pg/ml)	29.23 ± 7.7	24.52 ± 6.63	0.63

Plasma was isolated from fasting rats and used in the following analyses: Glucose-trinder (glucose); Radioimmunoassay (adiponectin, corticosterone, estradiol, total testosterone, free testosterone); and Enzyme-linked immunosorbent assay (insulin, leptin).